

Calculations of Electron Inelastic Mean Free Paths in Solids over the 10 eV to 200 keV Energy Range with the Relativistic Full Penn Algorithm

H. Shinotsuka¹, S. Tanuma², C. J. Powell³, and D. R. Penn³

¹ *Advanced Algorithm & Systems, Co. Ltd.*

² *National Institute for Materials Science (NIMS)*

³ *National Institute of Standards and Technology (NIST)*

1. Introduction

2. Calculation of IMFPs from optical data

- IMFP calculation with relativistic full Penn algorithm
- Evaluation of energy-loss function
- Fano Plots : relativistic modified Bethe equation
- Comparison of IMFPs with the relativistic TPP-2M equation

3. Comparison of calculation model for IMFPs

- Full Pen algorithm, Single pole approximation, Mermin-type ELF (Denton approach), Lindhard ELF approach

4. Comparison of IMFPs from EPES experiments

5. Summary

1. Introduction

- The electron inelastic mean free path (IMFP) is a basic material parameter for describing the surface sensitivity of AES, XPS and other surface electron spectroscopies.
- growing interest in XPS and related experiments performed with X-rays of much higher energies for both scientific and industrial purposes. (up to 30keV)
- a need for IMFPs at higher energy region in transmission electron microscopy. (up to 200 or 300 KeV)

We have started to extend the IMFP calculations over 10 eV to 200 keV using relativistic full Penn algorithm (FPA) from ELFs for 41 elemental solids and 30 compound semiconductors.

2. Calculation of IMFPs from optical data

- IMFP calculation with relativistic full Penn algorithm

:Relativistic DCS (< 0.5 MeV; Fernandez-Varea)

$$\frac{d^2\sigma}{d\omega dq} = \frac{d^2\sigma_L}{d\omega dq} + \frac{d^2\sigma_T}{d\omega dq} \approx \frac{d^2\sigma_L}{d\omega dq} = \frac{2}{\pi N v^2} \text{Im} \left(\frac{-1}{\varepsilon(q, \omega)} \right) \frac{1}{q}$$

: Probability $P(T, \omega)$ for energy loss per unit distance traveled by an electron with relativistic kinetic energy T .

$$p(T, \omega) = \frac{(1 + T/c^2)^2}{1 + T/(2c^2)} \frac{1}{\pi T} \int_{q_-}^{q_+} \frac{dq}{q} \text{Im} \left[\frac{-1}{\varepsilon(q, \omega)} \right]$$

$$q_{\pm} = \sqrt{T(2 + T/c^2)} \pm \sqrt{(T - \omega)(2 + (T - \omega)/c^2)}$$

$$\lambda(T) = 1 / \int_0^{\omega_{\max}} p(T, \omega) d\omega$$

Full Penn Algorithm for ELF calculation

The ELF in the FPA can be expressed as:

$$\text{Im} \left[\frac{-1}{\varepsilon(q, \omega)} \right] = \int_0^\infty d\omega_p g(\omega_p) \text{Im} \left[\frac{-1}{\varepsilon^L(q, \omega; \omega_p)} \right] \quad \leftarrow \text{Lindhard ELF}$$

$$g(\omega) = \frac{2}{\pi\omega} \text{Im} \left[\frac{-1}{\varepsilon(\omega)} \right] \quad \leftarrow \text{Optical ELF (measured)}$$

$$\text{Im} \left[\frac{-1}{\varepsilon^L(q, \omega; \omega_p)} \right] = \frac{\varepsilon_2^L}{(\varepsilon_1^L)^2 + (\varepsilon_2^L)^2}$$

$$\varepsilon_1^L(q, \omega; \omega_p) = 1 + \frac{1}{\pi k_F z^2} \left[\frac{1}{2} + \frac{1}{8z} \left\{ F\left(z - \frac{x}{4z}\right) + F\left(z + \frac{x}{4z}\right) \right\} \right]$$

$$\varepsilon_2^L(q, \omega; \omega_p) = \frac{1}{8k_F z^3} \times \begin{cases} x & \text{for } 0 < x < 4z(1-z) \\ 1 - (z - (x/4z))^2 & \text{for } |4z(1-z)| < x < 4z(1+z), \\ 0 & \text{otherwise} \end{cases}$$

Conditions and materials for IMFP calculations

Energy range for IMFP calculations: 10 eV to 200 keV

- calculated at equal intervals on a logarithmic energy scale corresponding to increases of 10 %.

Energy range of ELF's for materials: 0.1 eV - 1MeV

- 41 elemental solids

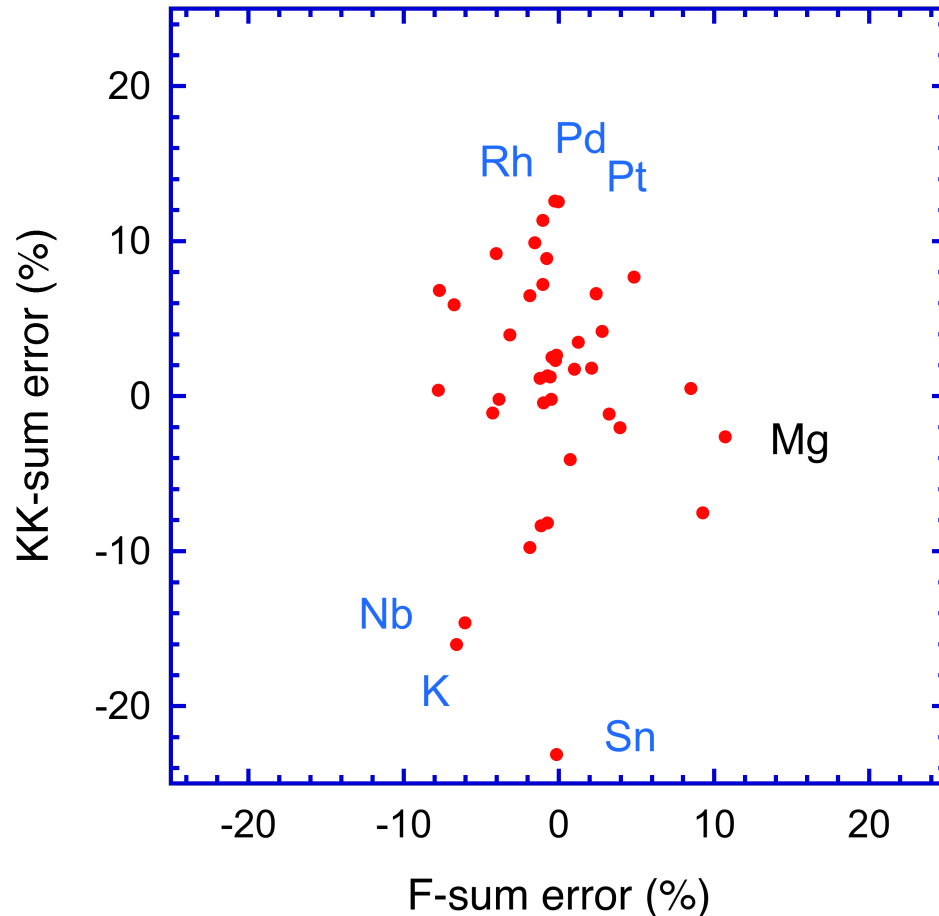
Li, Be, diamond, graphite, glassy carbon, Na, Mg, Al, Si, K, Sc, Ti, V, Cr, Fe, Co, Ni, Cu, Ge, Y, Nb, Mo, Ru, Rh, Pd, Ag, In, Sn, Cs, Gd, Tb, Dy, Hf, Ta, W, Re, Os, Ir, Pt, Au, and Bi.

-30 compound semiconductors

AgBr, AgCl, AgI, AlAs, AlN, AlSb, BN, BN(hex), CdS, CdSe, CdSe(hex), CdTe, GaAs, GaN, GaP, GaSb, GaSe, InAs, InP, InSb, PbS, PbSe, PbTe, SiC, SiC(hex), SnTe, ZnS, ZnS(hex), ZnSe, ZnTe

Evaluation of ELF_s (0 - 1 MeV) : elemental solids

41 elemental solids



- F-sum : One solid is slightly larger than 10 % (Mg) .
- KK-sum : 6 solids are larger than 10 % error (K, Nb, Rh, Pd, Sn, and Pt).
- the sum-rule errors for **K** and **Nb** are both of the same sign (negative in each case), indicating that their ELF_s are systematically too small and thus their calculated IMFPs will be too large.
- For 34 of our 41 elemental solids, the f-sum-rule and KK-sum rule errors are both less than 10 %.

ELFs : compound semiconductor

- Experimental ELFs or optical constants are lacking over 10 eV.
- Optical Constants and ELFs for 30 compound semiconductors were calculated with FEFF8.2 and WIEN2K in 0.1 eV – 1 MeV.

FEFF: Automated program to calculate the X-ray absorption spectra based on an ab initio all-electron, real space relativistic Green's function formalism

→ Available for inner-shell electron excitation

WIEN2K: Program package to perform the electron structure calculation based on density functional theory using full potential and linearized augmented plane wave method

→ Available for valence electron excitation

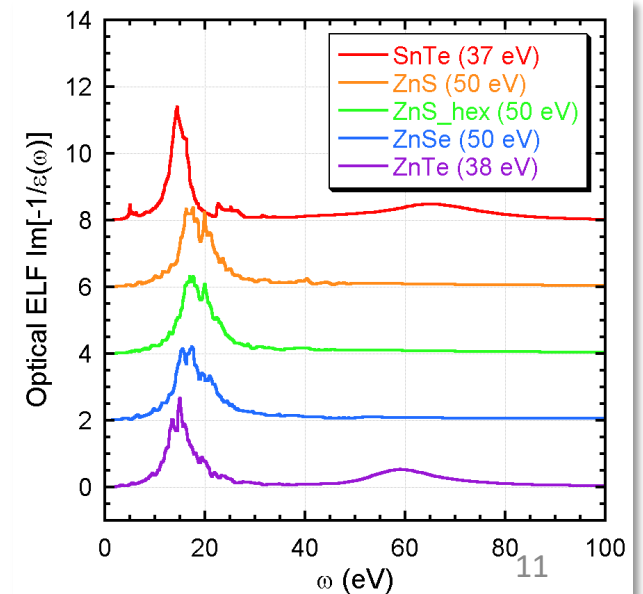
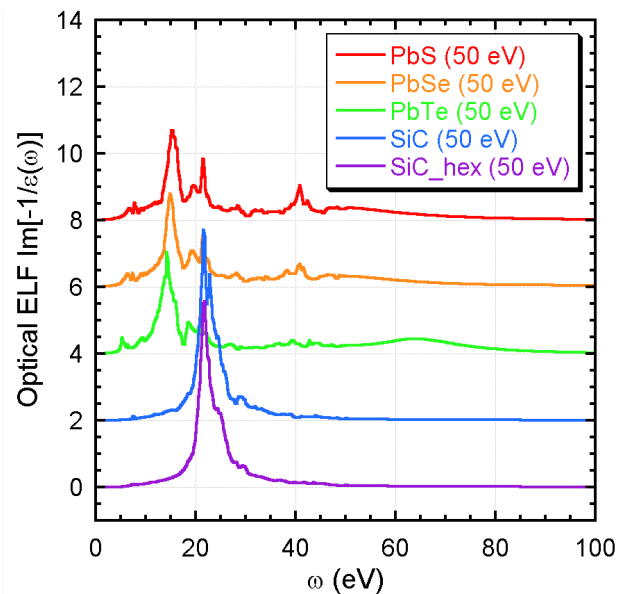
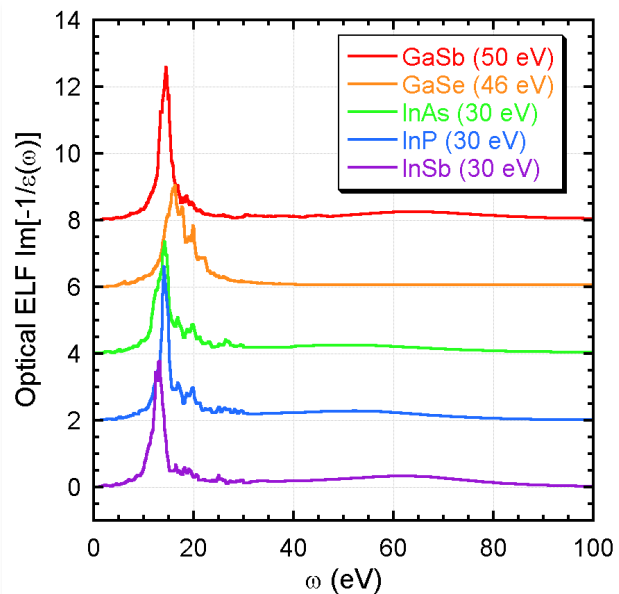
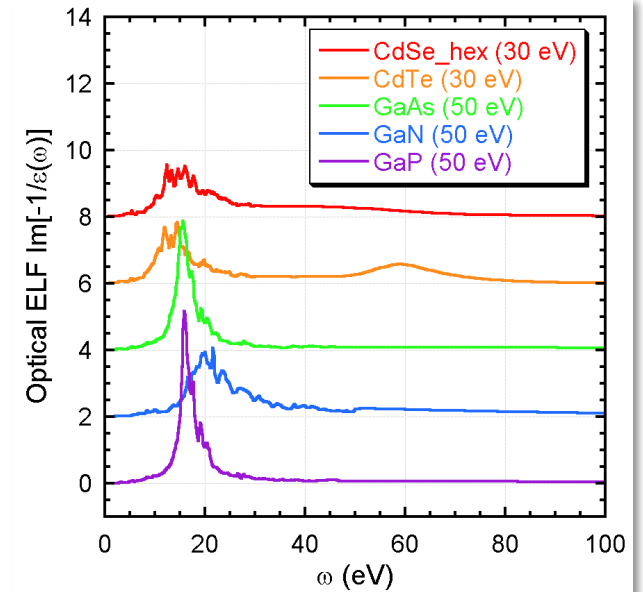
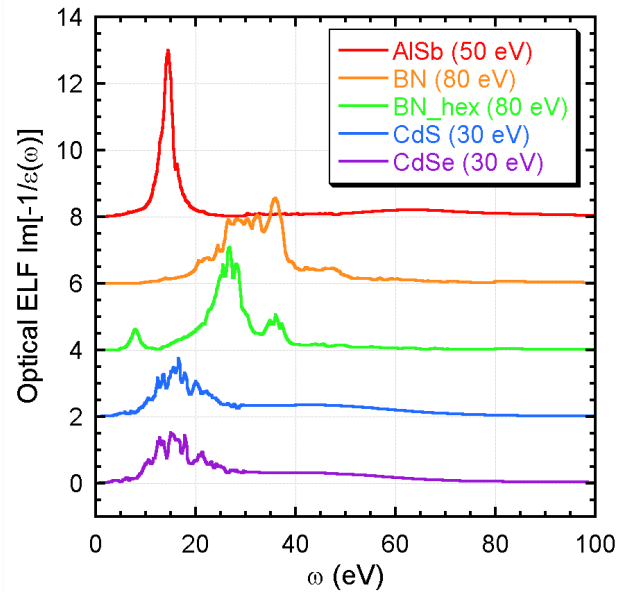
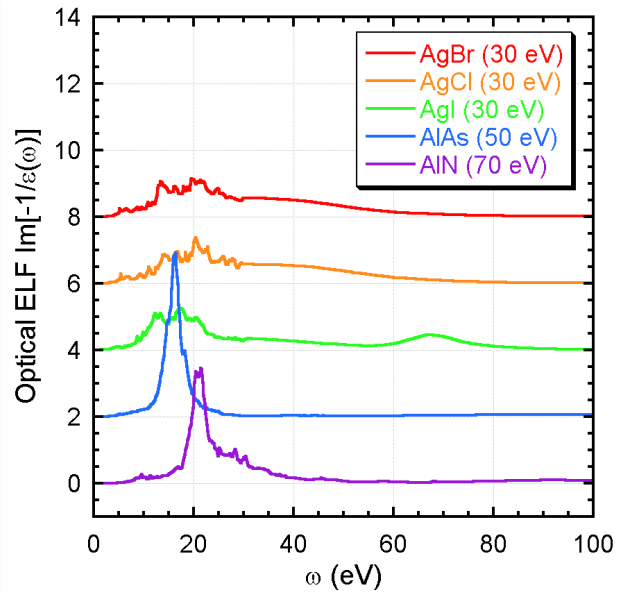
- Space group and cell parameters : ex. AgBr , F m -3 m, a = 5.775

List of 30 semiconductors calculated

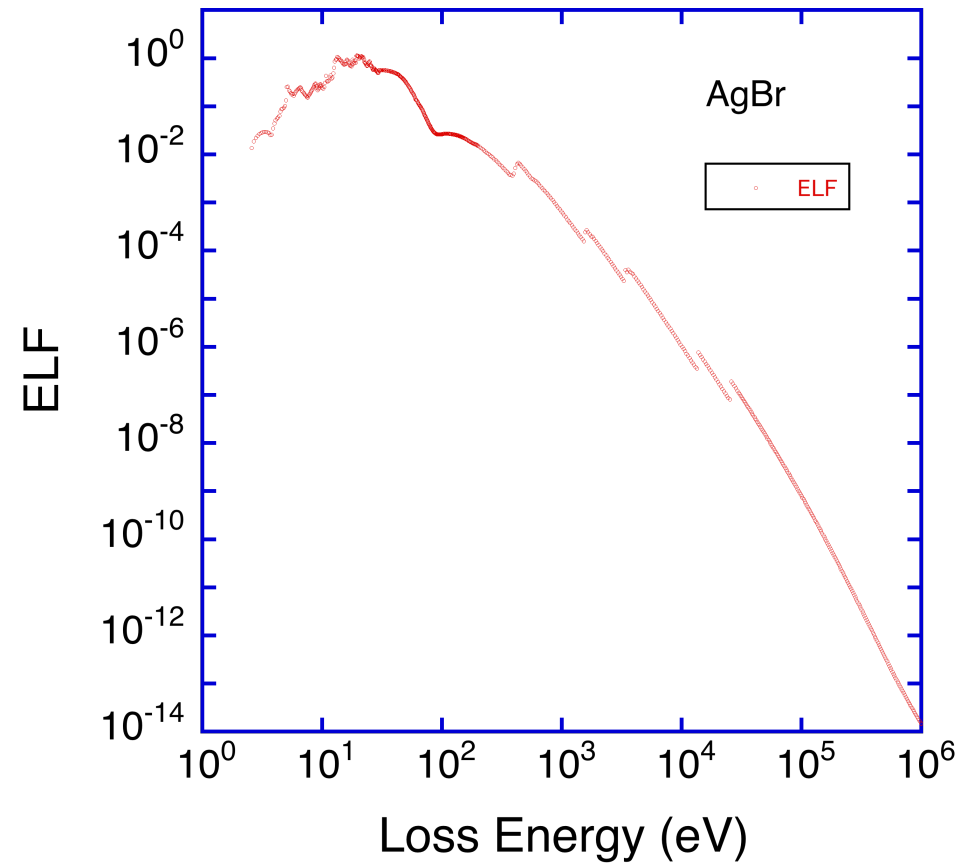
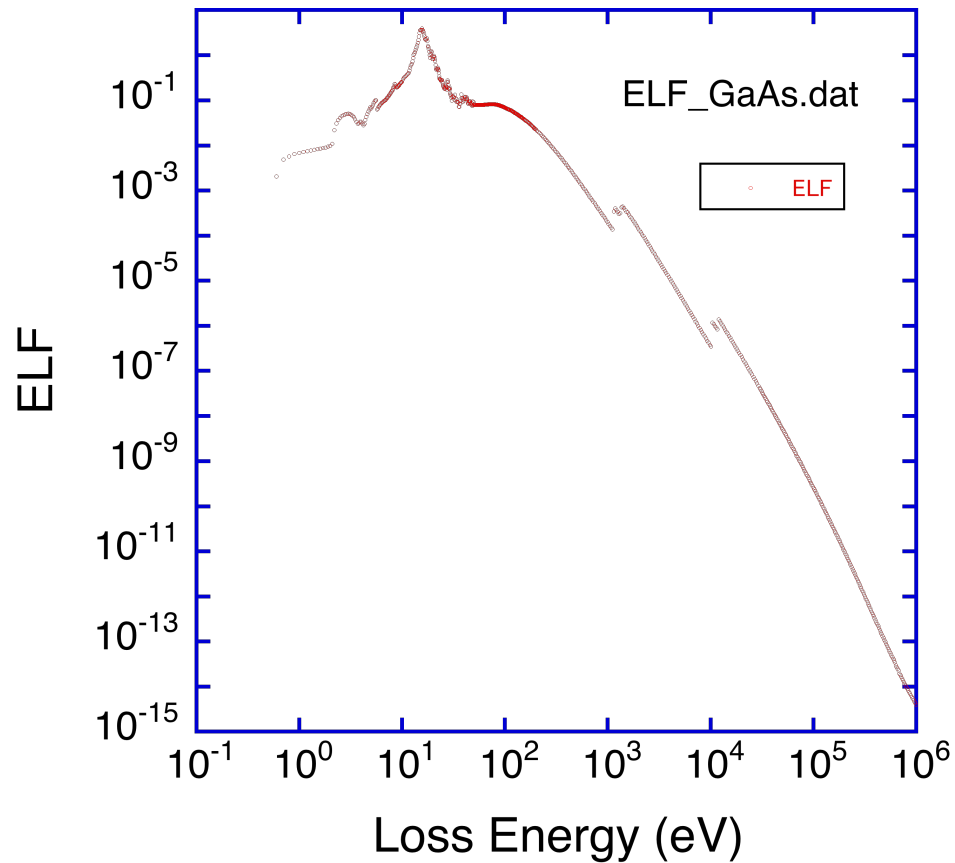
Material	Space Group	Cell parameter (angstrom or degree)
AgBr	F m -3 m	a = 5.775
AgCl	F m -3 m	a = 5.543
AgI	P 63 m c	a = 4.5856 c = 7.49 g = 120
AlAs	F -4 3 m	a = 5.6605
AlN	P 63 m c	a = 3.11 c = 4.98 g = 120
AlSb	F -4 3 m	a = 6.135
BN	F -4 3 m	a = 3.6159
BN_hex	P 63 /mmc	a = 2.5045 c = 6.606 g = 120
CdS	P 63 m c	a = 4.142 c = 6.724 g = 120
CdSe	F -4 3 m	a = 6.04
CdSe_hex	P 63 m c	a = 4.299 c = 7.01 g = 120
CdTe	F -4 3 m	a = 6.482
GaAs	F -4 3 m	a = 5.6532

Material	Space Group	Cell parameter (angstrom or degree)
GaN	P 63 m c	a = 3.1891 c = 5.1855 g = 120
GaP	F -4 3 m	a = 5.4508
GaSb	F -4 3 m	a = 6.0959
GaSe	P 63 /mmc	a = 3.75 c = 15.995 g = 120
InAs	F -4 3 m	a = 6.0577
InP	F -4 3 m	a = 5.8687
InSb	F -4 3 m	a = 6.4794
PbS	F m -3 m	a = 5.9315
PbSe	F m -3 m	a = 6.1213
PbTe	F m -3 m	a = 6.4541
SiC	F -4 3 m	a = 4.3581
SiC_hex	P 63 m c	a = 3.076 c = 5.048 g = 120
SnTe	F m -3 m	a = 6.323
ZnS	F -4 3 m	a = 5.4102
ZnS_hex	P 63 m c	a = 3.822 c = 6.26 g = 120
ZnSe	F -4 3 m	a = 5.6692
ZnTe	F -4 3 m	a = 6.1026

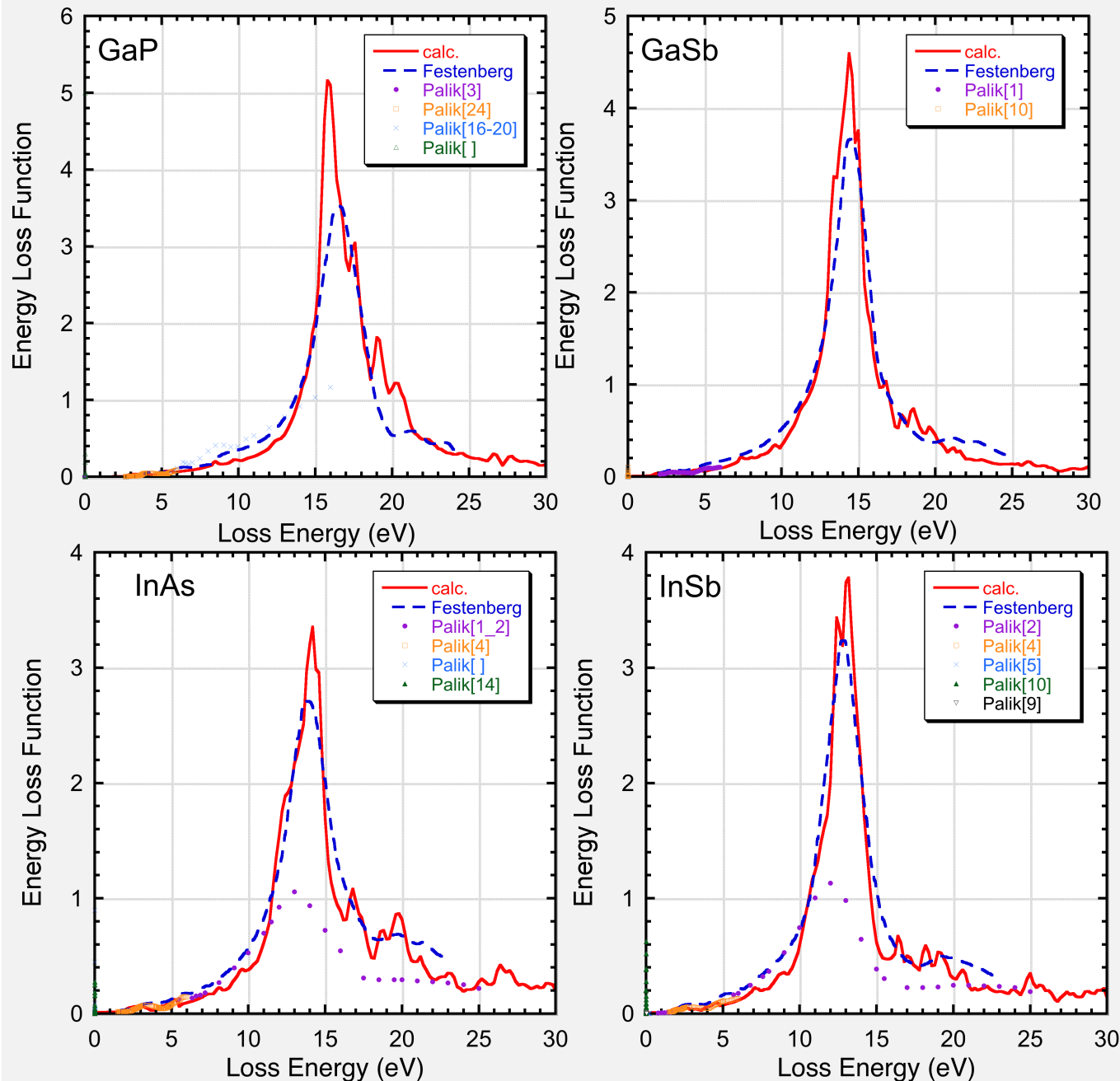
Calculated results of ELF for 30 compounds



ELS for GaAs and AgBr



Comparison of ELFs with Palik data and TEM-EELS



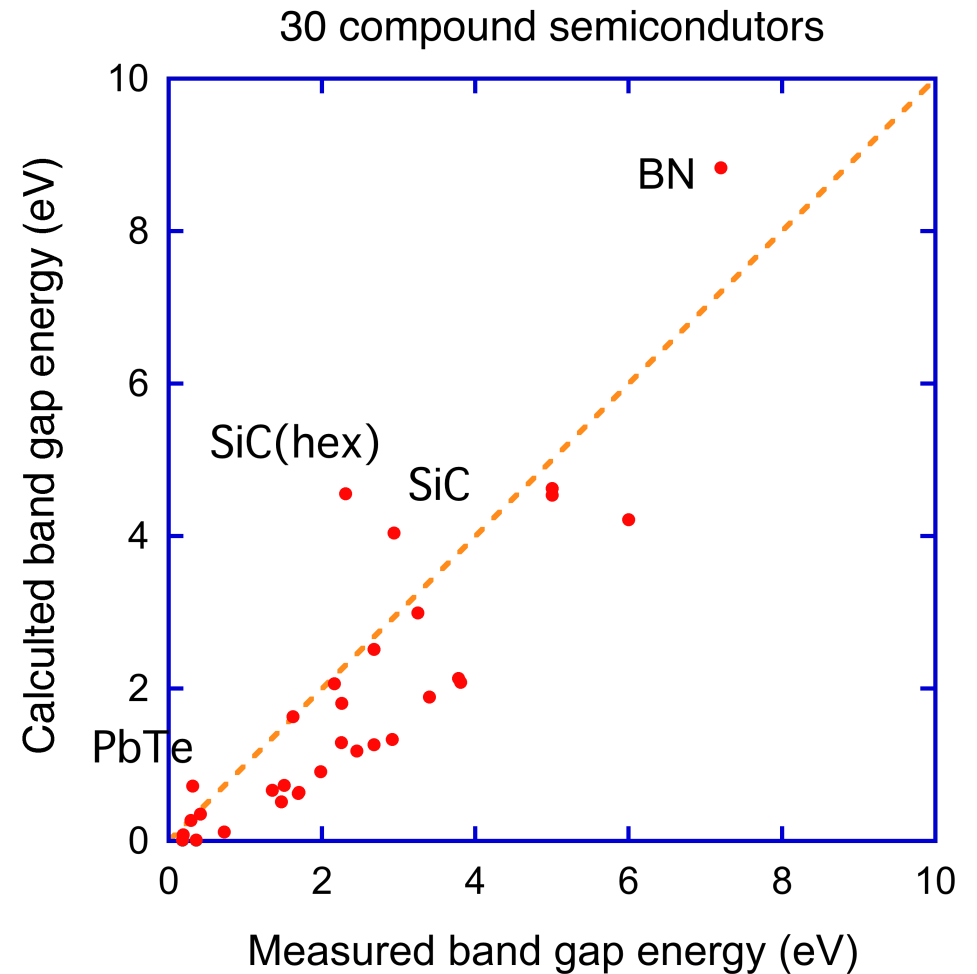
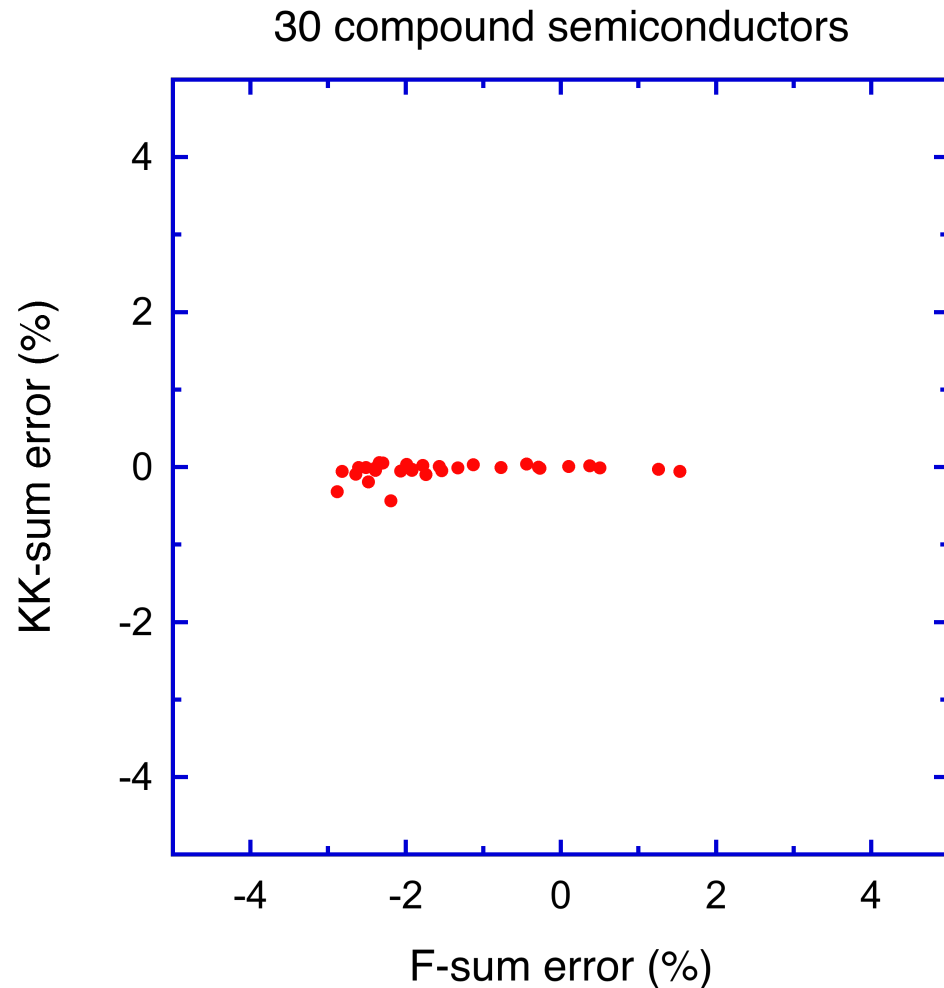
: good agreement
Wien2k - TEM

: poor >10 eV (InAs, InSb)
Wien2k – Palik data

: comparison with REELS
for GaAs

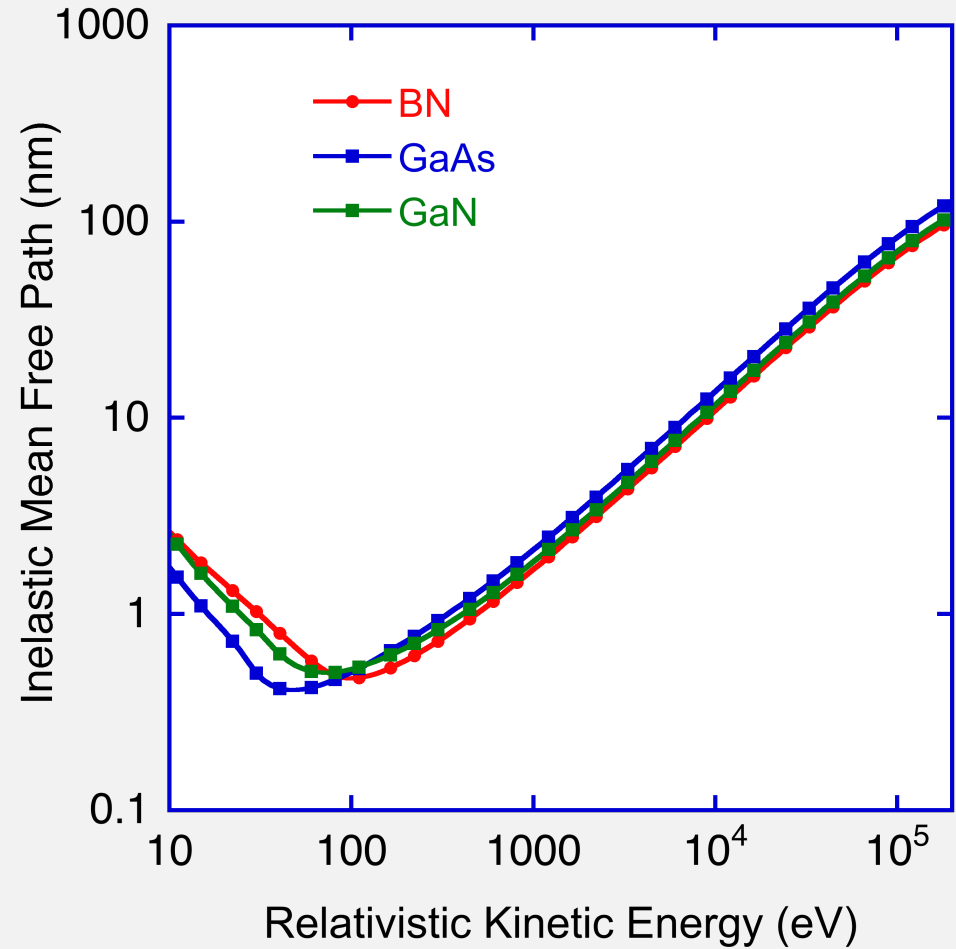
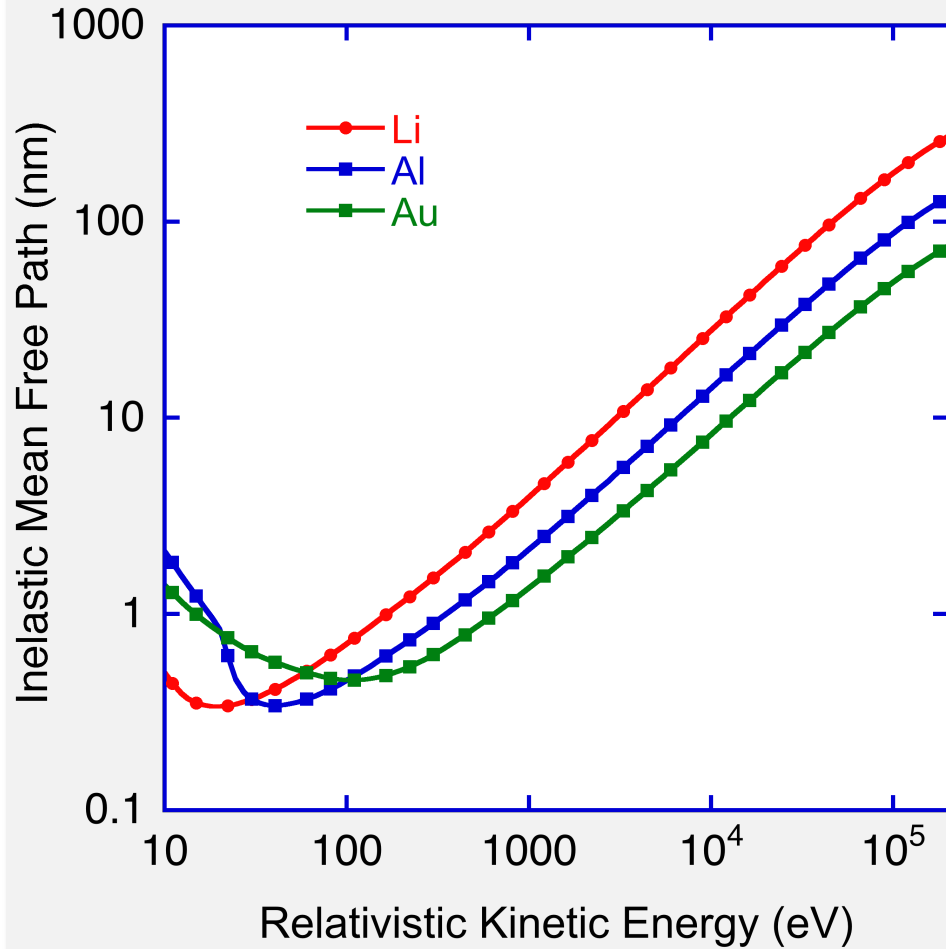
➔ Yoshikawa-san
on Thursday

Evaluation of ELF's : 30 compound semiconductors



Calculated E_g : estimated from calculated ELF's
Measured E_g : median value in the references

Calculated results of IMFPs : 10 eV – 200keV



Relativistic TPP-2M eq. and Fano Plot

$$\sigma_{tot} = \frac{4\pi a_0^2 z^2}{mv^2 / 2R} \left\{ M_{tot}^2 \left[\ln \left(\frac{4c_{tot} mv^2}{R \cdot 2} \right) - \ln(1 - B^2) - B^2 \right] \right\}$$

$$B = \frac{v}{c}$$

Relativistic Bethe equation by Inokuti

Non-relativistic Bethe equation

$$\sigma_{tot}^{non-rel} = \frac{4\pi a_0^2 z^2}{E/R} \left\{ M_{tot}^2 \left[\ln \left(\frac{4c_{tot} E}{R} \right) \right] + \frac{g_n}{E/R} + O \left(\frac{h_n}{E^2} \right) \right\}$$

$$\lambda^{non-rel} = \frac{0.1 \times E}{E_p^2 \left\{ \beta \ln(\gamma E) - C/E + D/E^2 \right\}} \quad (\text{nm})$$

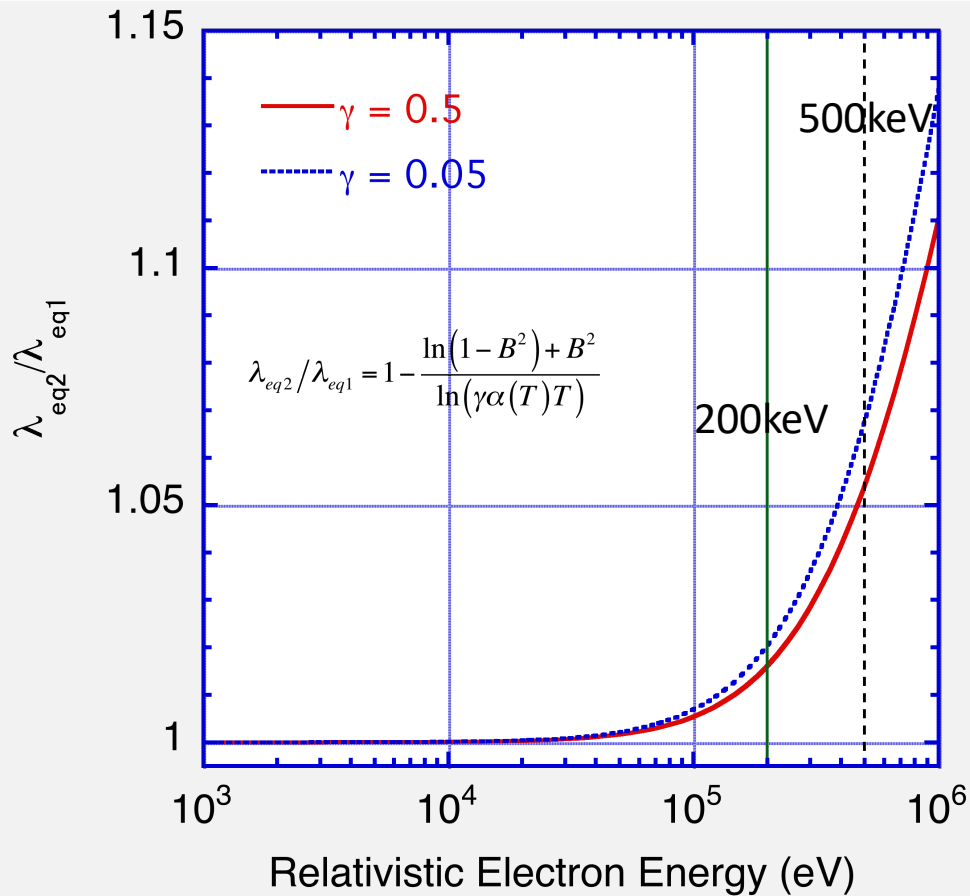
$$\lambda = \frac{0.1 \times \alpha(T) T}{E_p^2 \left\{ \beta \left[\ln(\gamma \alpha(T) T) - \ln(1 - B^2) - B^2 \right] - C/T + D/T^2 \right\}} \quad (\text{nm})$$

$$\alpha(T) = \frac{1 + T / (2m_e c^2)}{\left[1 + T / (m_e c^2) \right]^2}$$

Relativistic Fano plot : $0.1 \times \alpha(T) T / \lambda$ vs. $\left[\ln(\alpha(T) T) - \ln(1 - B^2) - B^2 \right]$

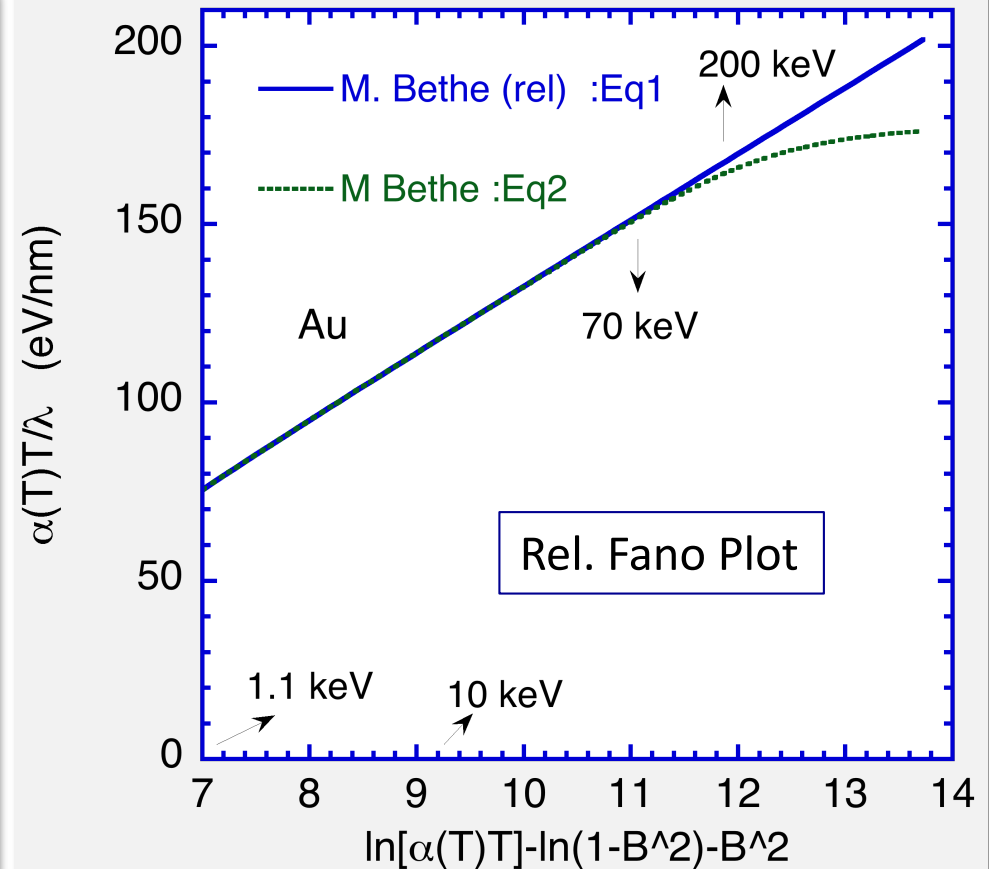
Straight line at high energy region : γ = slope

Comparison of eq.1 and 2 on Fano plot



Eq.1

$$\lambda_{eq1} = \frac{0.1 \times \alpha(T)T}{E_p^2 \left\{ \beta \left[\ln(\gamma\alpha(T)T) - \ln(1-B^2) - B^2 \right] - C/T + D/T^2 \right\}}$$



Eq.2

Original M. Bethe eq. form

$$\lambda_{eq2} = \frac{0.1 \times \alpha(T)T}{E_p^2 \left\{ \beta \ln(\gamma\alpha(T)T) - C/T + D/T^2 \right\}}$$

Fano plots of Au over 1keV – 1MeV

:Relativistic DCS

longitudinal excitation

transverse excitation

$$\frac{d^2\sigma}{d\omega dq} = \frac{d^2\sigma_L}{d\omega dq} + \frac{d^2\sigma_T}{d\omega dq}$$

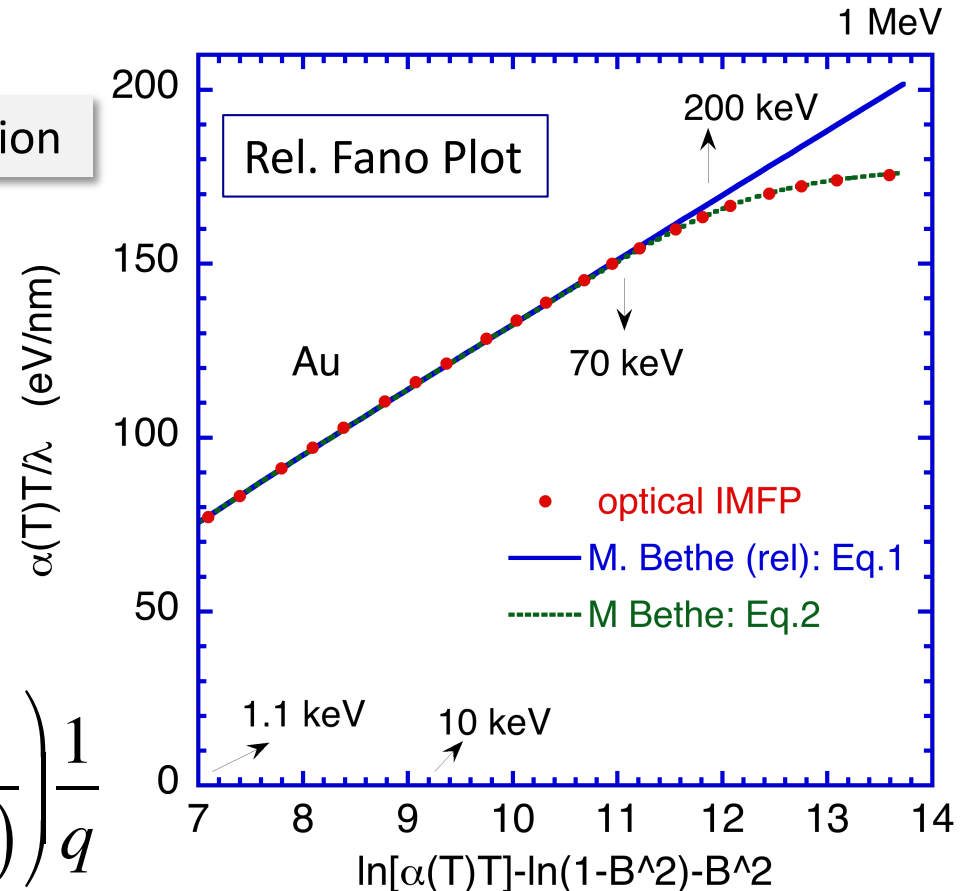
$$\lambda = 1/n\sigma$$

< 0.5 MeV

$$\frac{d^2\sigma}{d\omega dq} \simeq \frac{d^2\sigma_L}{d\omega dq} = \frac{2}{\pi N v^2} \text{Im} \left(\frac{-1}{\varepsilon(q, \omega)} \right) \frac{1}{q}$$

Eq.1

$$\lambda_{eq1} = \frac{0.1 \times \alpha(T)T}{E_p^2 \left\{ \beta \left[\ln(\gamma \alpha(T)T) - \ln(1-B^2) - B^2 \right] - C/T + D/T^2 \right\}}$$

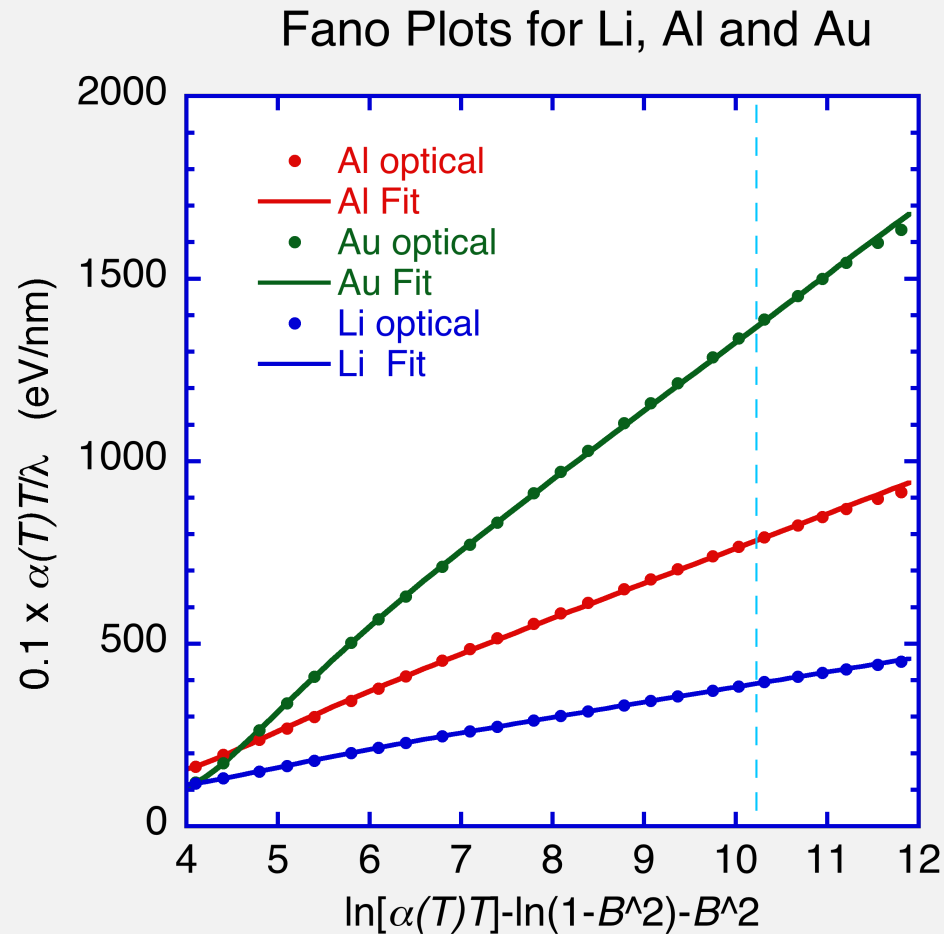


Eq.2

Original M. Bethe eq. form

$$\lambda_{eq2} = \frac{0.1 \times \alpha(T)T}{E_p^2 \left\{ \beta \ln(\gamma \alpha(T)T) - C/T + D/T^2 \right\}}$$

Fano plots and Curve fits for 3 elemental solids



Solid circles: calculated from IMFPs
(rel. FPA method)

Solid lines: Fit with Rel. mod. Bethe
equation

Energy range: 50 eV – 200 keV

RMS differences (%)

Li : 0.43

Al : 0.98

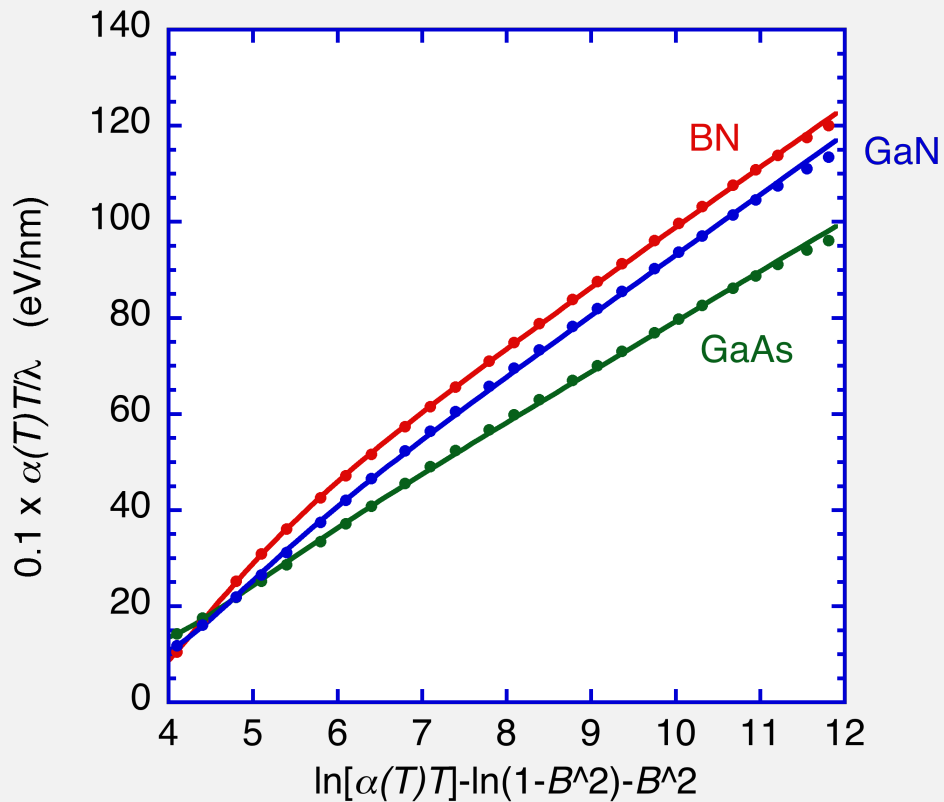
Au : 0.59

Average of RMS (%) for
41 elemental solids

0.82% (0.4 – 1.4 %)

$$\frac{0.1 \times \alpha(T)T}{\lambda} = E_p^2 \left\{ \beta \left[\ln(\gamma \alpha(T)T) - \ln(1 - B^2) - B^2 \right] - C/T + D/T^2 \right\} \quad (\text{nm/eV})$$

Fano plots and Curve fits for 3 semiconductors



Solid circles: calculated from IMFPs
(rel. FPA method)

Solid lines: Fit with Rel. mod. Bethe
equation

Energy range: 50 eV – 200 keV

RMS differences (%)

BN : 0.58

GaN : 1.1

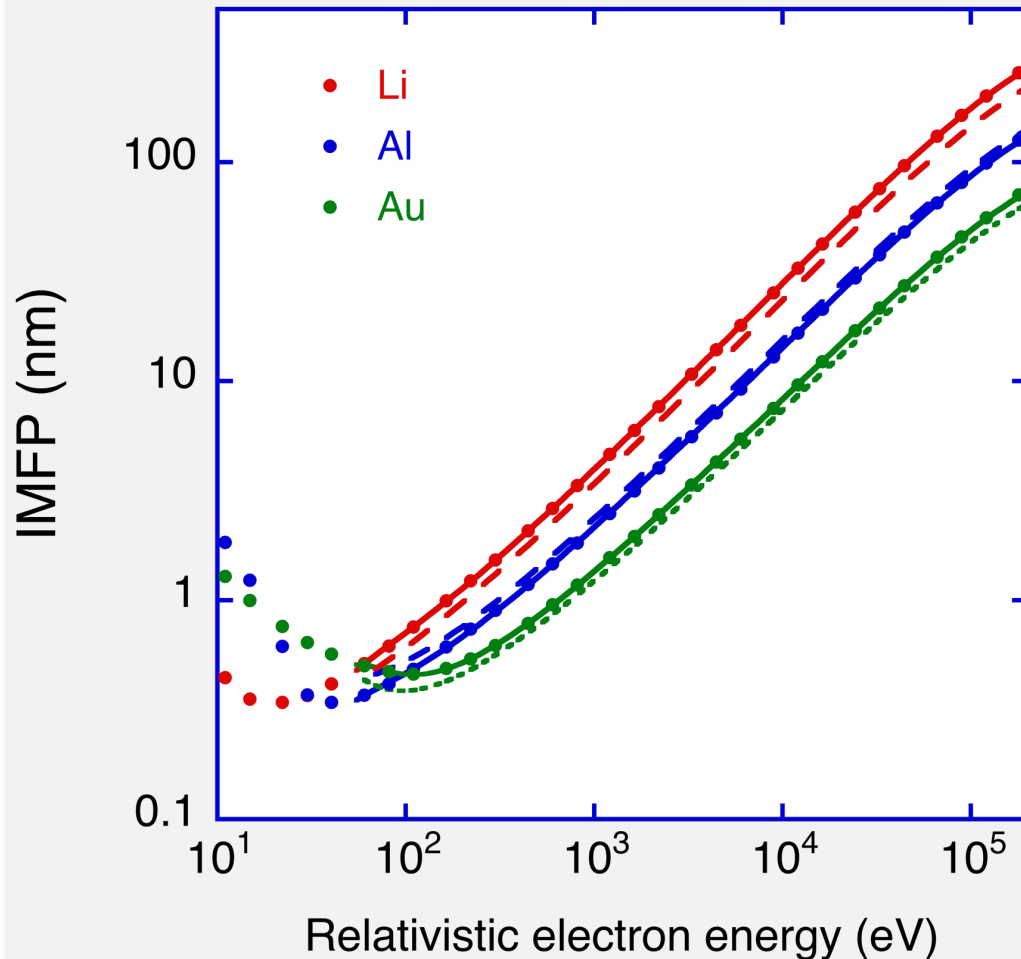
GaAs : 1.1

Average of RMS (%) for 30 compounds

0.74 % (0.4 – 1.1 %)

$$\frac{0.1 \times \alpha(T)T}{\lambda} = E_p^2 \left\{ \beta \left[\ln(\gamma \alpha(T)T) - \ln(1 - B^2) - B^2 \right] - C/T + D/T^2 \right\} \quad (\text{nm/eV})$$

Comparison of IMFPs with rel. TPP-2M for 3 elemental solids



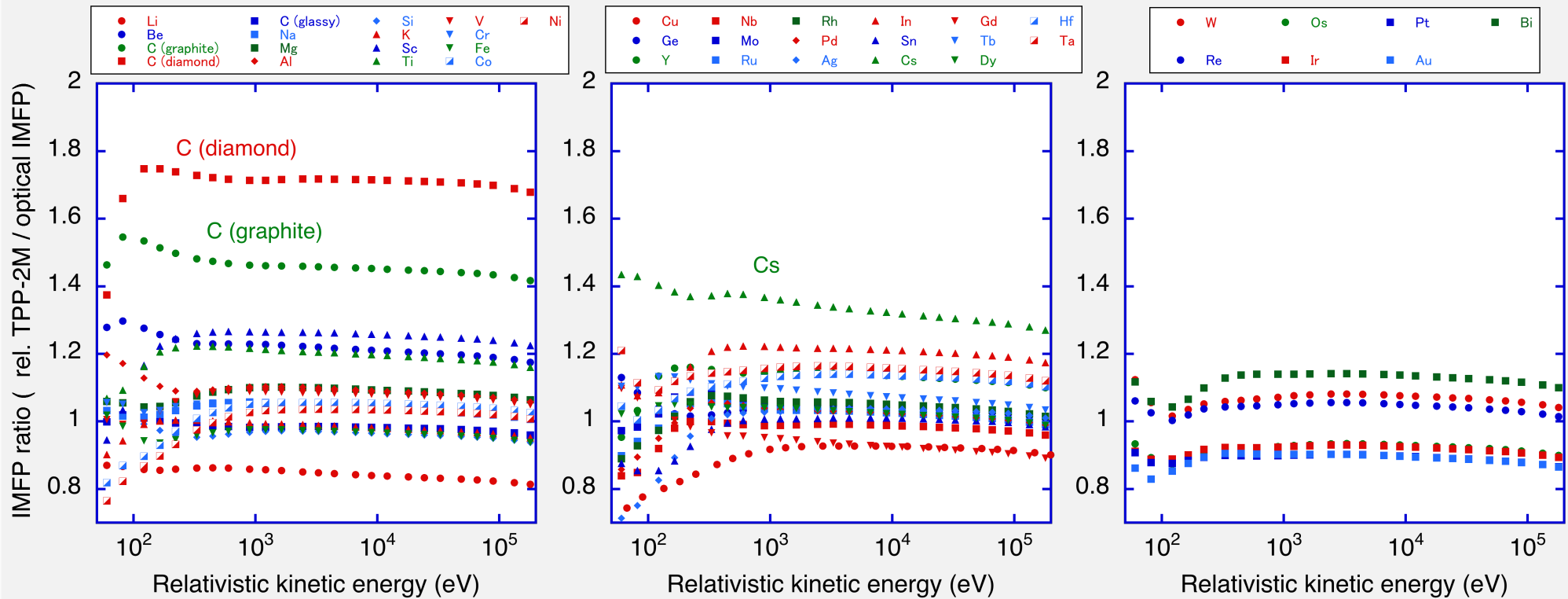
Solid circles: calculated with rel. FPA
Solid lines: Fit with Rel. M. Bethe eq.
Dotted lines: rel. TPP-2M

Energy range: 50 eV – 200 keV
RMS differences (%) for rel. TPP-2M

Li	: 15.5
Al	: 10.2
Au	: 11.4

Average of RMS (%) for
41 elemental solids : 11.9 %

Ratios of IMFPs for 41 elemental solids

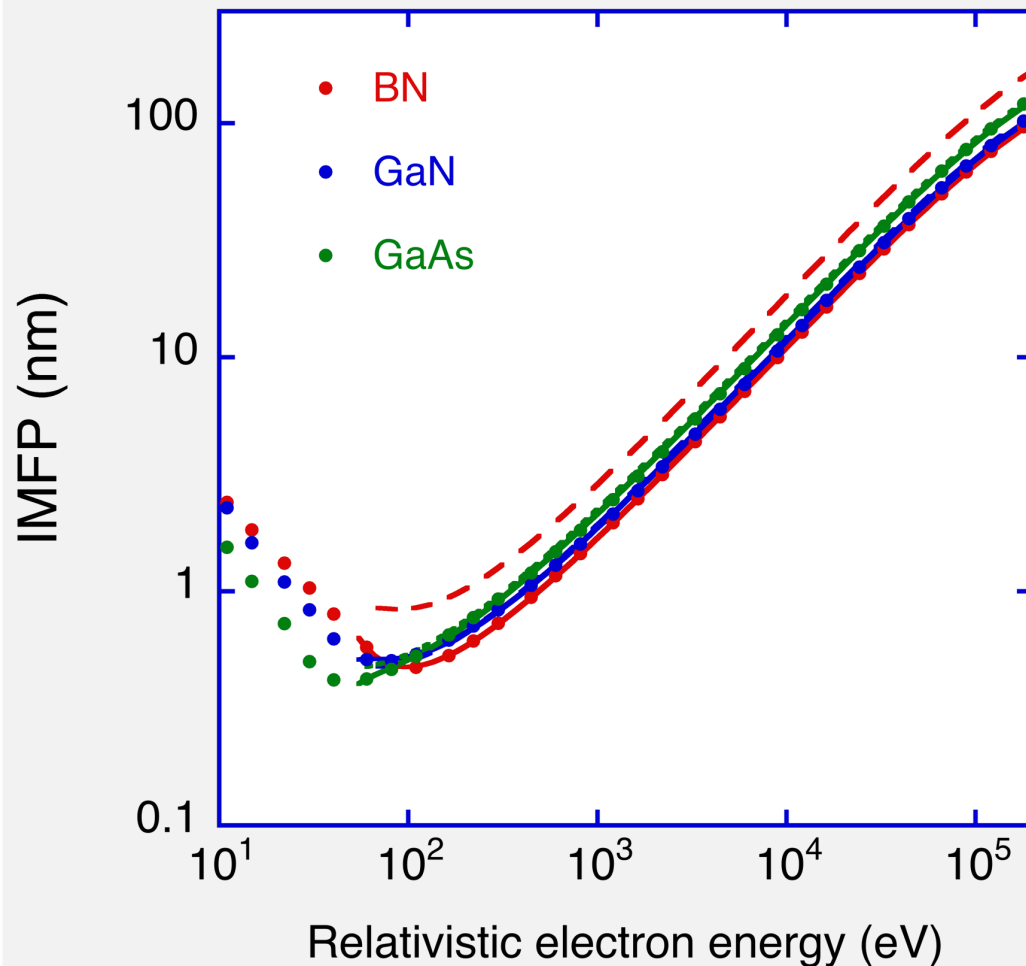


Average of RMS (%) for 41 elemental solids

11.9 % (2.0 – 70 %) : 41 solids

8.9 % (except for diamond, graphite, Cs)

Comparison of IMFPs with rel TPP-2M for 3 compounds



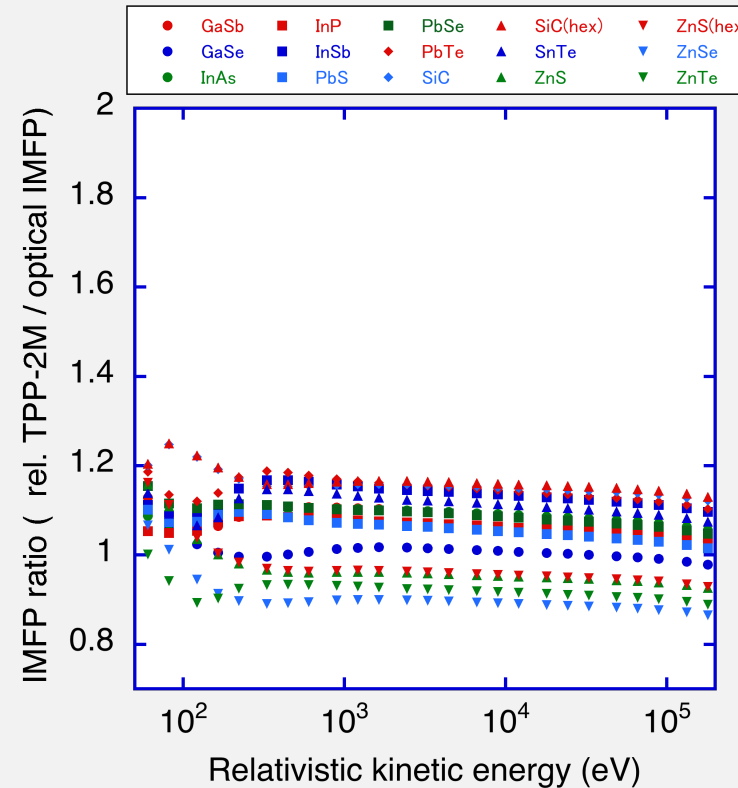
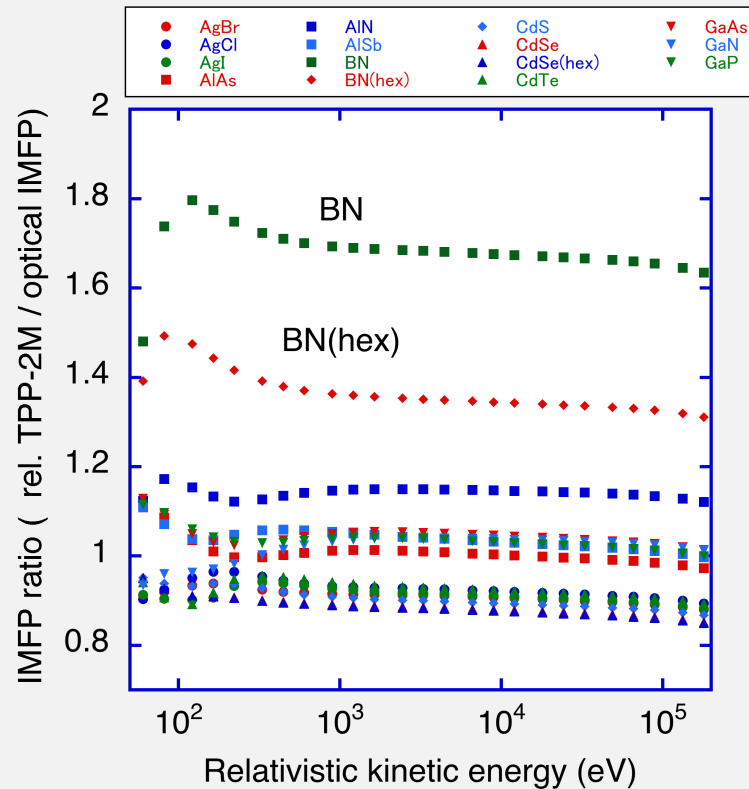
Solid circles: calculated with rel. FPA
Solid lines: Fit with Rel. M. Bethe eq.
Dotted lines: rel. TPP-2M

Energy range: 50 eV – 200 keV
RMS differences (%) for rel. TPP-2M

BN	: 68.6
GaN	: 3.4
GaAs	: 5.0

Average of RMS (%) for
30 compound semiconductors
: 11.7 %

Ratios of IMFPs for 30 compound semiconductors



Average of RMS (%) for compound semiconductors
11.7 % (2.4 – 69 %) : 30 materials
8.8 % (except BN)

Electron exchange effect on IMFP calculation

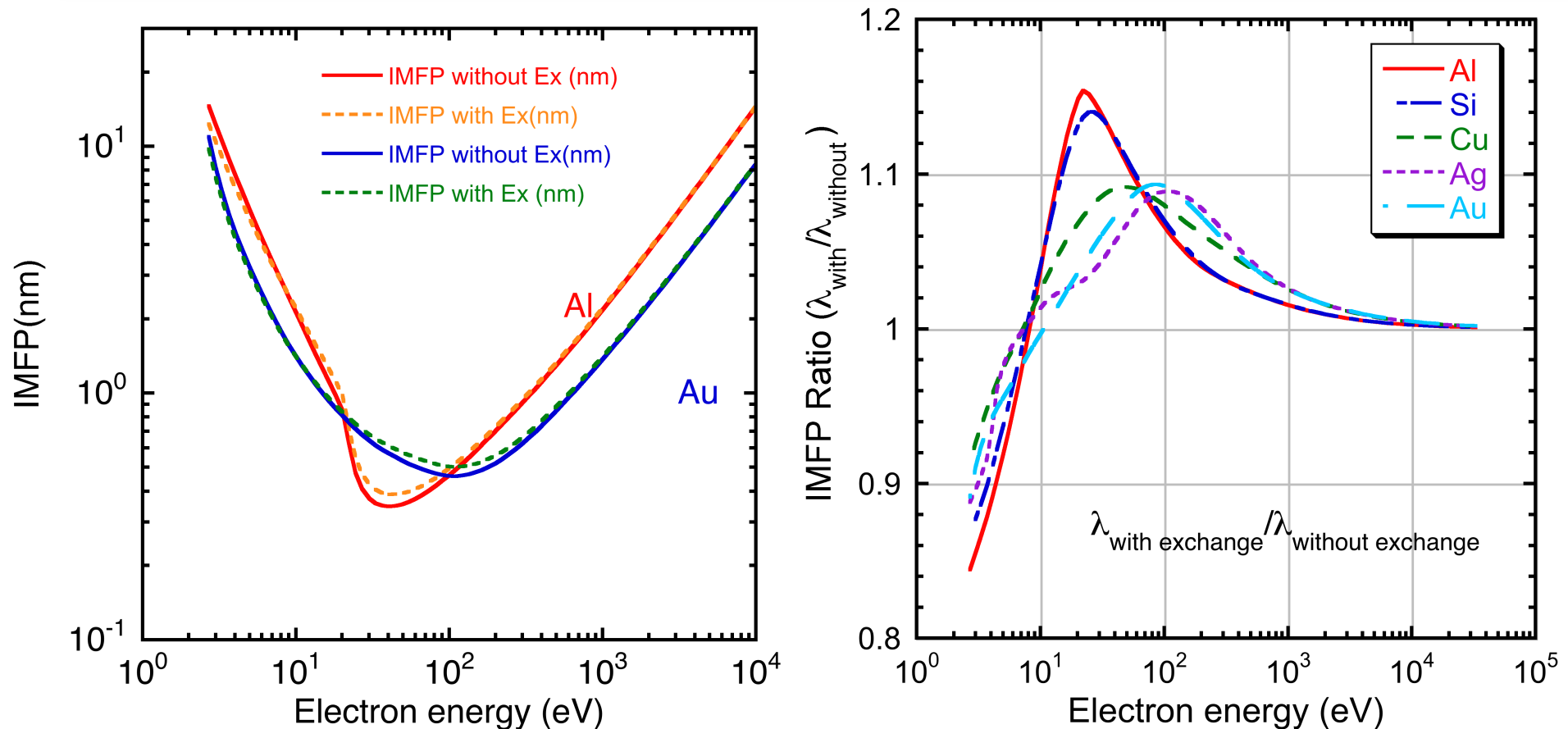
- important to know the effect of exchange between projectile and target electrons on IMFP calculations with the FPA.
- no consensus on how to incorporate exchange effects within the dielectric formalism
- estimate the influence of electron exchange on IMFPs using the Born-Ochkur exchange correction.

The non-relativistic DCS with the Born-Ochkur correction can be written as (Fernandez-Varea *et al.*)

$$\frac{d^2\sigma}{dq d\omega} = \left(1 - \frac{q^2}{2E} + \left(\frac{q^2}{2E} \right)^2 \right) \frac{1}{\pi N E} \operatorname{Im} \left[\frac{-1}{\varepsilon(q, \omega)} \right] \frac{1}{q}$$

-calculated IMFPs of **Al, Si, Cu, Ag, and Au** with and without the exchange correction and compared them.

Influence of electron exchange on IMFPs



- IMFPs with the exchange correction are larger than those without the exchange correction for Al and Au between 10 eV and 30 000 eV.

- Above 100 eV, the difference between IMFPs with and without exchange correction are less than about 10% for these elemental solids.

- Born-Ochkur corr. is essentially a high-energy approximation. It is then not clear whether this approximation is useful for evaluating the exchange correction for energies less than 100 eV.

Comparison of ELF for Al : Mermin, Lindhard model

1) Mermin model (ELF at q=0)

$$\text{Im} \left[\frac{-1}{\varepsilon^D(q=0, \omega; \omega_p; \gamma)} \right] = \frac{\gamma \omega \omega_p^2}{(\omega^2 - \omega_p^2)^2 + (\gamma \omega)^2}$$

- Used data for Al ELF (valence)

ω_p (eV)	γ (eV)	A
15	0.95	1

$$\varepsilon_M(q, \omega) = 1 + \frac{1 + i\gamma / \omega}{\left[\varepsilon_L(q, \omega + i\gamma) - 1 \right]^{-1} + (i\gamma / \omega) \left[\varepsilon_L(q, 0) - 1 \right]^{-1}} = 1 + \frac{1 + i\gamma / \omega}{A/f + (i\gamma / \omega) A}$$

2) Lindhard model (ELF at q=0)

$$\text{Im} \left[\frac{-1}{\varepsilon^L(q=0, \omega; \omega_p; \gamma)} \right] = \frac{2\gamma \omega \omega_p^2}{(\omega^2 - \omega_p^2 - \gamma^2)^2 + (2\gamma \omega)^2}$$

$$\varepsilon_L(q, \omega) = 1 + \frac{f}{A}$$

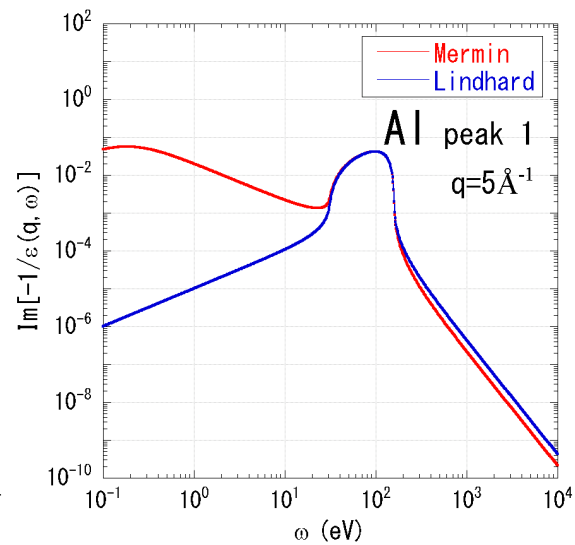
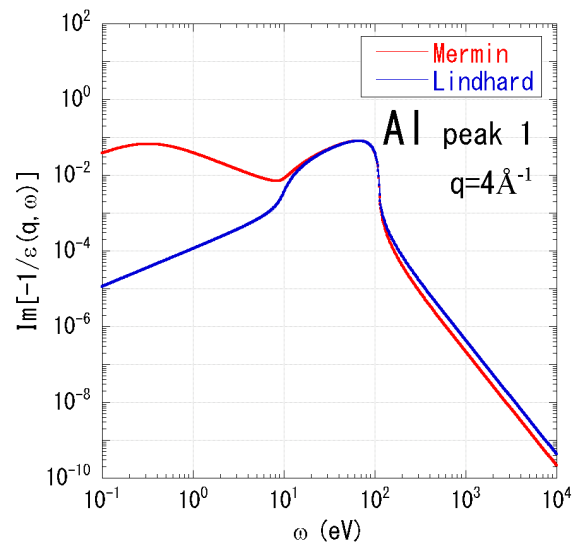
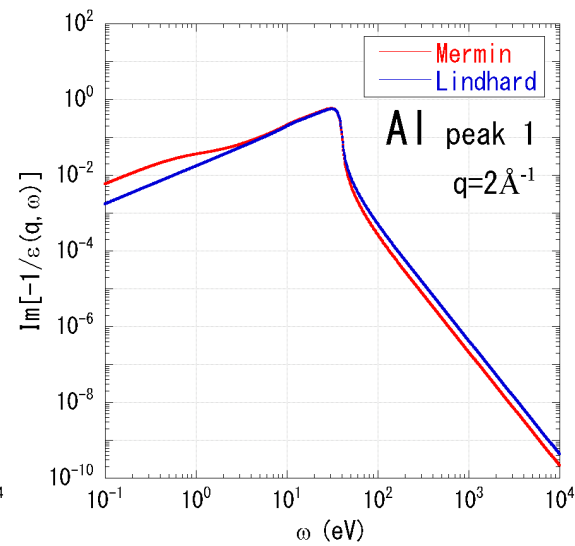
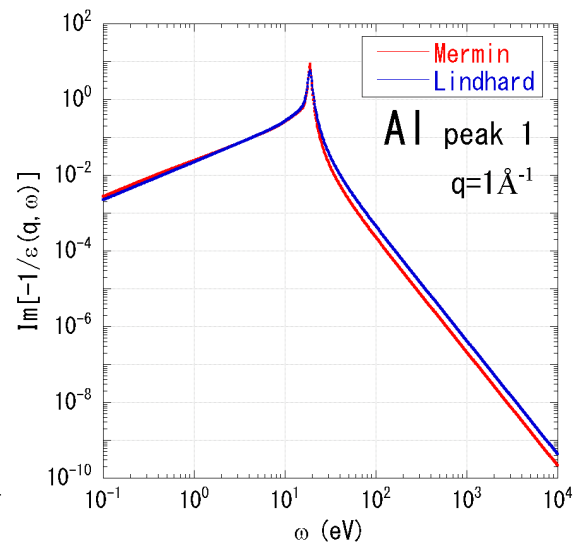
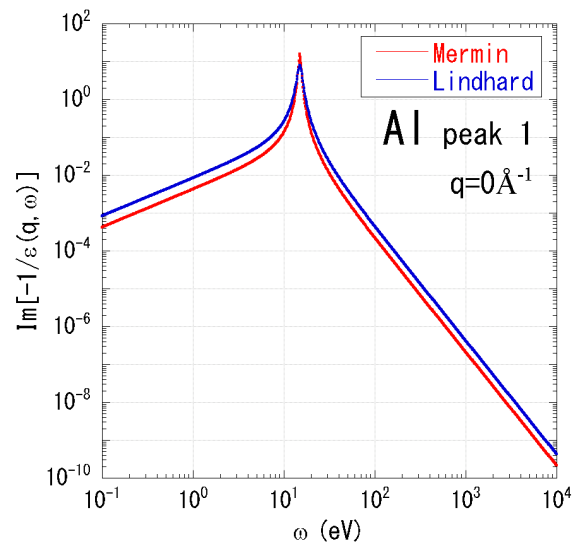
$$A \equiv \left[\varepsilon_L(q, 0) - 1 \right]^{-1} = (qv_F / \omega_p)^2 / 3$$

$$D \equiv \left[\varepsilon_L(q, \omega + i\gamma) - 1 \right]^{-1} = A / f$$

$$f = \frac{1}{2} + \frac{1}{8z} \left\{ 1 - (z - u') \right\}^2 \ln \frac{z - u' + 1}{z - u' - 1} + \frac{1}{8z} \left\{ 1 - (z + u') \right\}^2 \ln \frac{z + u' + 1}{z + u' - 1}$$

$$z = q / 2k_F, \quad u' = \omega' / kv_F, \quad \omega' = \omega + i\gamma$$

Comparison of ELF for Al : Mermin, Lindhard model



Comparison of ELF for Al : Mermin, Lindhard, FPA, and SPA

1) Mermin model (ELF at q=0)

n= 2 ; Valence and L-shell

$$\text{Im} \left[\frac{-1}{\varepsilon(q=0, \omega)} \right] = \sum A_i \text{Im} \left[\frac{-1}{\varepsilon^M(q=0, \omega; \omega_{p,i}; \gamma_i)} \right]_{\omega \geq \omega_{th,i}}$$

Al	EF=11.2eV			
ω_p (eV)	γ (eV)	A	ω_{th} (eV)	
15	0.95		1	0
106.1	81.6		0.067	72.5

2) Lindhard model (ELF at q=0)

$$\text{Im} \left[\frac{-1}{\varepsilon(q=0, \omega)} \right]_{\text{Lindhard}} = \sum_i A_i \text{Im} \left[\frac{-1}{\varepsilon^L(q=0, \omega; \omega_{p,i}; \gamma_i)} \right]_{\omega \geq \omega_{th,i}}$$

3) FPA (ELF at q=0 : measured values)

FPA \neq Lindhard model

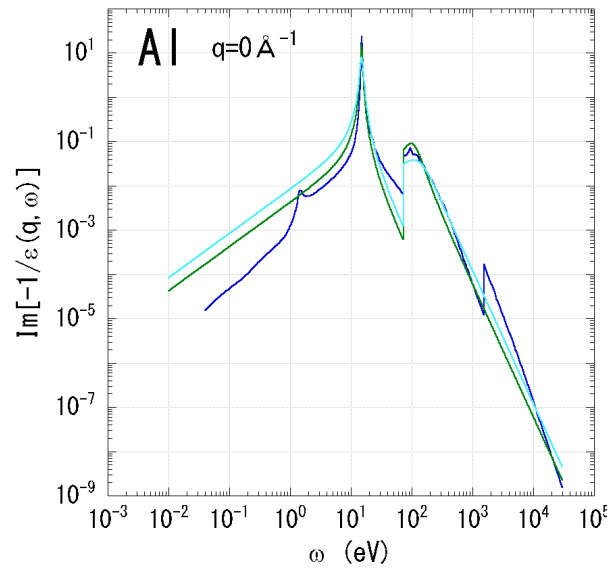
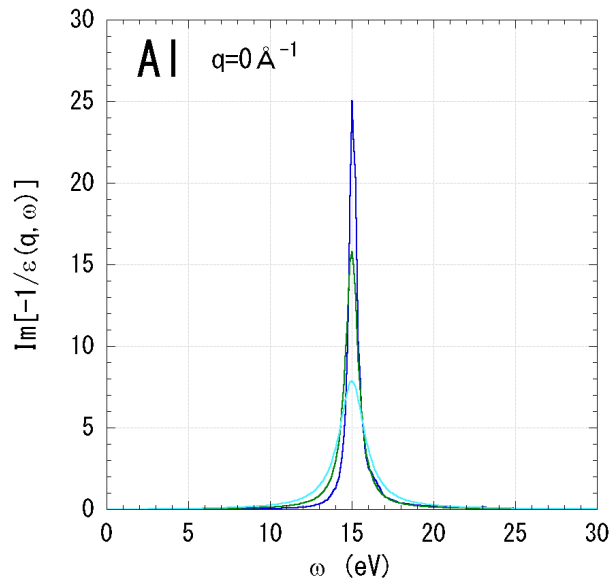
$$\text{Im} \left[\frac{-1}{\varepsilon(q, \omega)} \right] = \int_0^\infty d\omega_p g(\omega_p) \text{Im} \left[\frac{-1}{\varepsilon^L(q, \omega; \omega_p)} \right]$$

$$g(\omega) = \frac{2}{\pi\omega} \text{Im} \left[\frac{-1}{\varepsilon(\omega)} \right]$$

4) SPA with quartic dispersion eq. (ELF at q=0 : measured values)

$$\text{Im} \left[\frac{-1}{\varepsilon(q, \omega)} \right] = \text{Im} \left[\frac{-1}{\varepsilon(\omega_0)} \right] / \left\{ 1 + \frac{\pi q^2}{6k_F(\omega_0)} \right\}$$

Comparison of ELF's for Al : Mermin, Lindhard, SPA,FPA



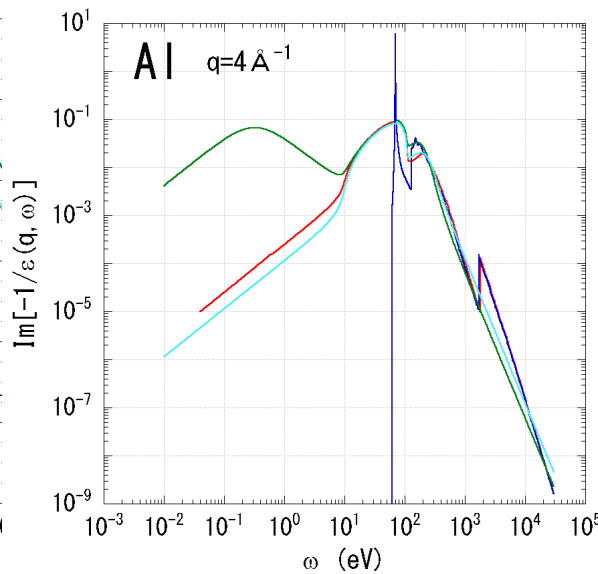
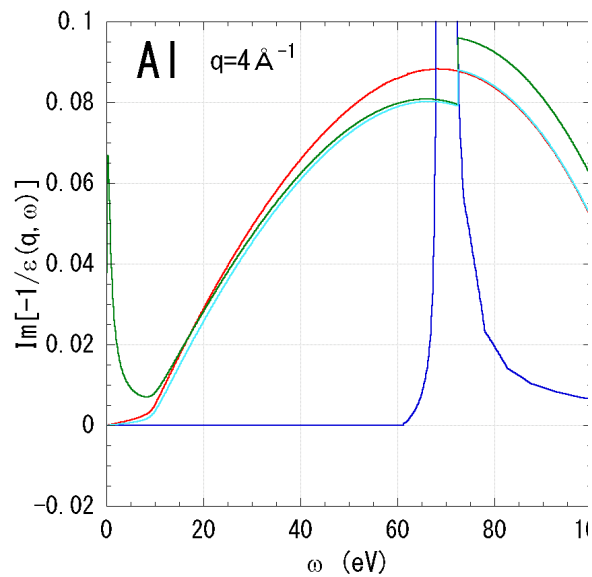
Red: FPA

Blue: SPA

Green: Mermin model

Light blue: Lindhard model

-FPA and Lindhard model show similar figures



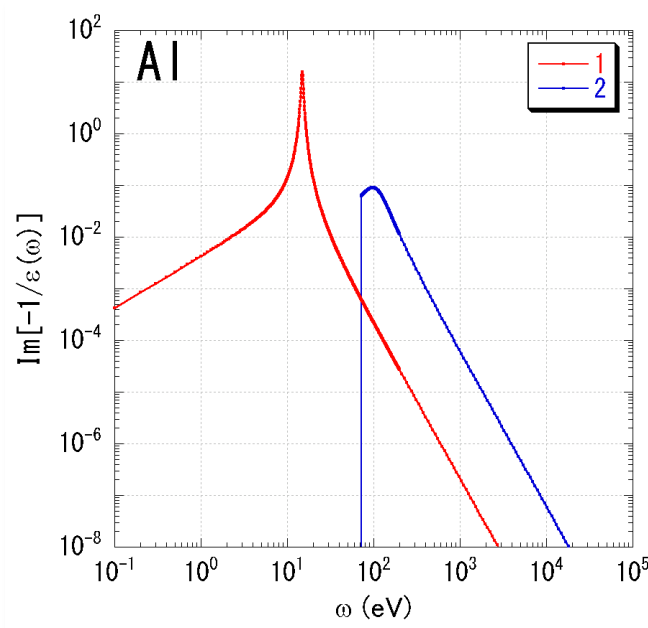
- a sharp edge or gap around 70 eV at $q=4$, this is due to the existence of the threshold energy of used ELF.

Problems in Mermin ELF approach

1. f-sum rule

- not satisfy at any q values due to W_{th}

$$\text{Im} \left[\frac{-1}{\epsilon(q=0, \omega)} \right]_{\text{valence}} = \sum_i A_i \text{Im} \left[\frac{-1}{\epsilon^M(q=0, \omega; \omega_i, \gamma_i)} \right]_{\omega \geq \omega_{th}}$$



Target	Entry	w_p (eV)	g (eV)	A	w_{th} (eV)
Al	1	15	0.95	1	0
$E_F=11.2\text{eV}$	2	106.1	81.6	0.067	72.5

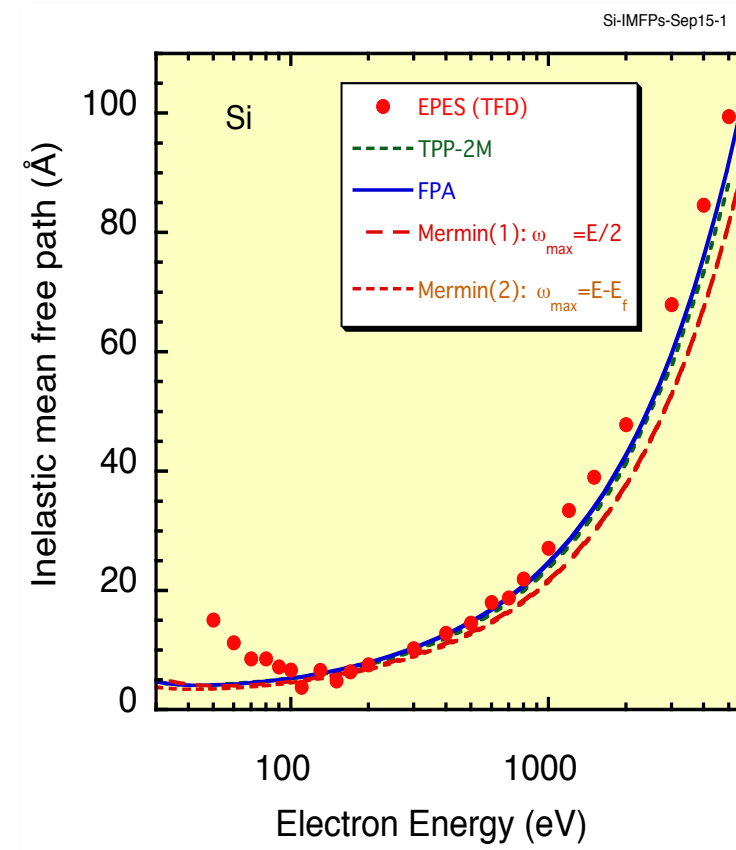
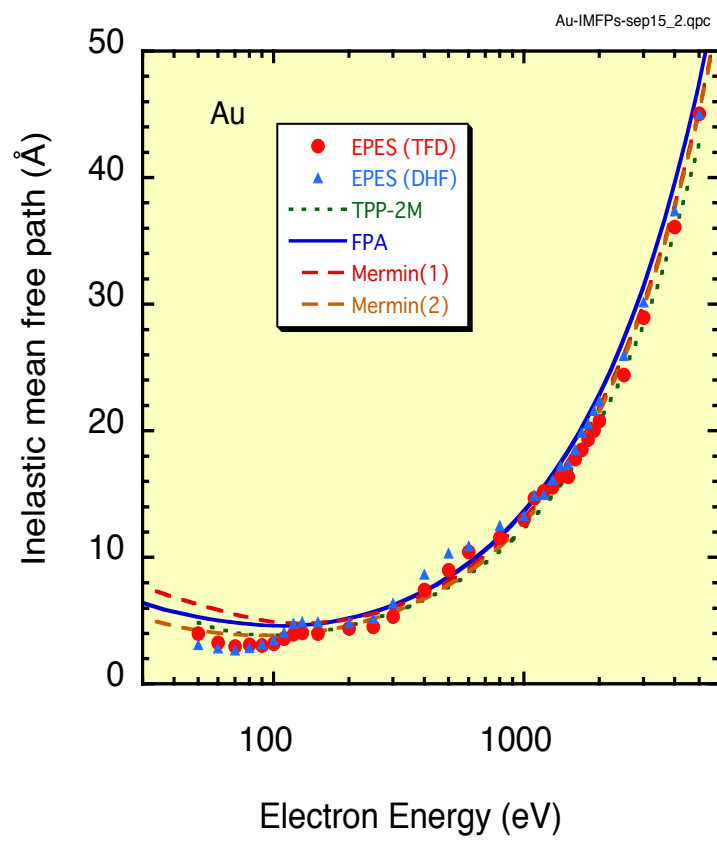
	$q=0 \text{ \AA}^{-1}$	$q=1 \text{ \AA}^{-1}$	$q=2 \text{ \AA}^{-1}$	$q=3 \text{ \AA}^{-1}$	$q=4 \text{ \AA}^{-1}$	$q=5 \text{ \AA}^{-1}$
Component 1	2.71	2.71	2.71	2.71	2.71	2.71
Component 2 with W_{th}	8.38	8.46	8.62	8.75	8.84	8.90
Neff (M and L shell)	11.09	11.17	11.33	11.46	11.55	11.61

2. Curve fit and separate calculation

- Curve fit of measured ELF with Drude function at $q=0$ for valence electron excitation
- GOS approach (Denton) for inner shell excitations

$$\text{Im} \left[\frac{-1}{\epsilon(q, \omega)} \right] = \text{Im} \left[\frac{-1}{\epsilon(q, \omega)} \right]_{\text{valence}} + \text{Im} \left[\frac{-1}{\epsilon(q, \omega)} \right]_{\text{inner-shell}}$$

4. Comparison of IMFPs from EPES experiments

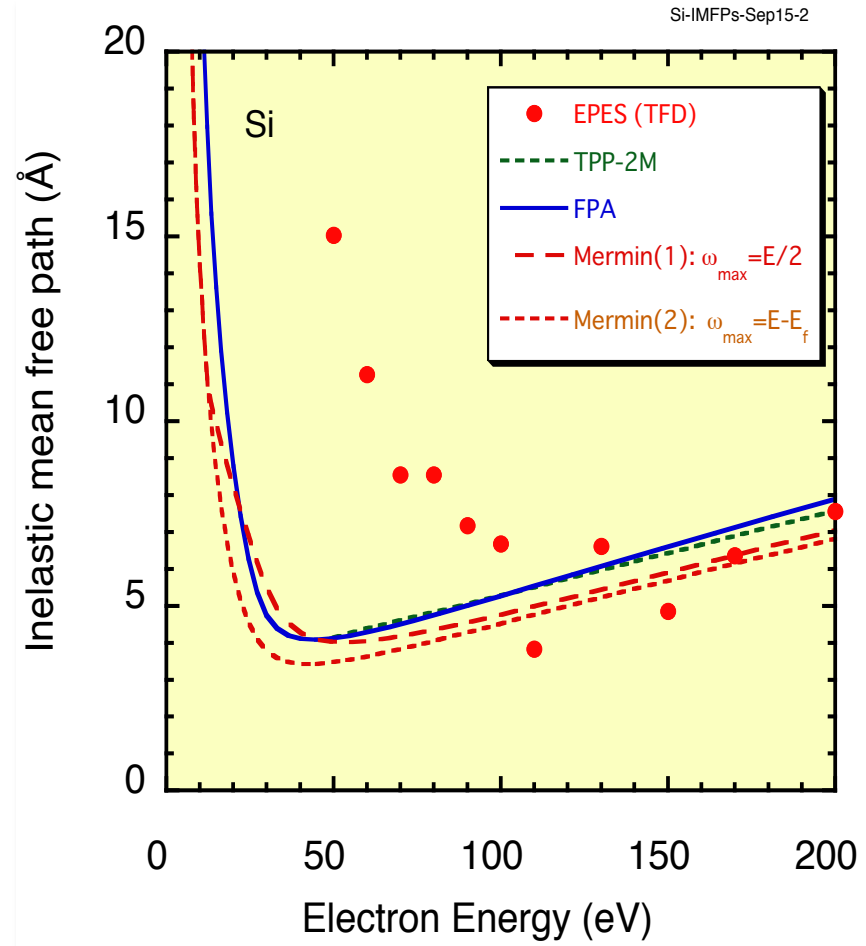
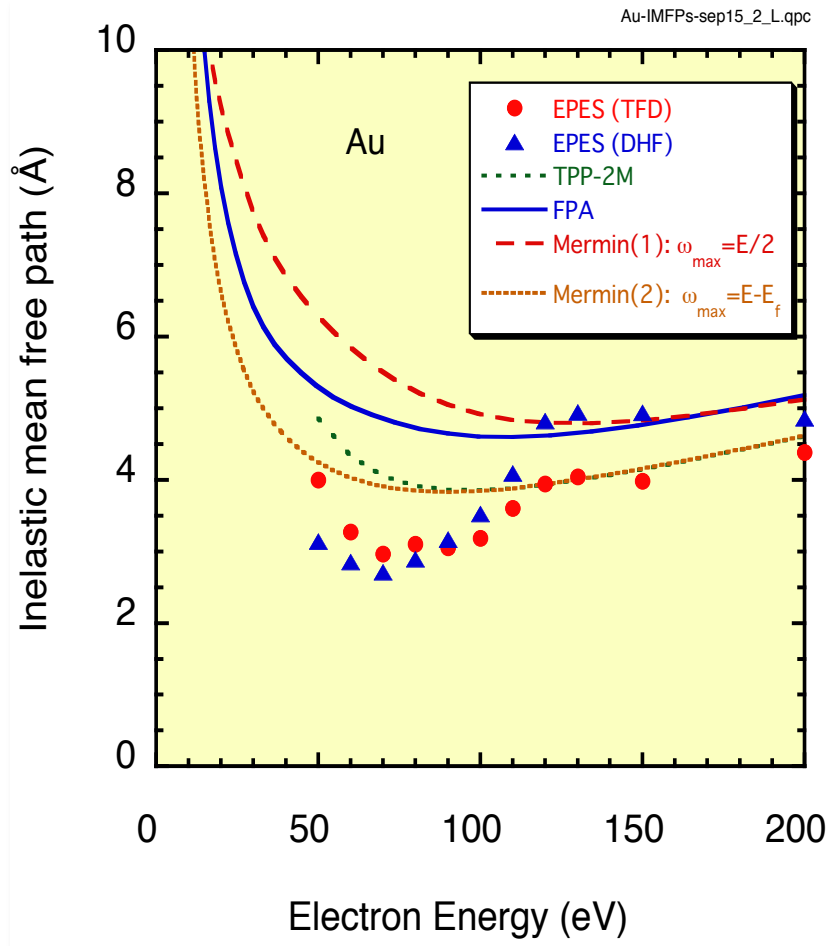


EPES: Ni-std

SEC: $f_s^x / f_s^{Ni} = 1$

$$\left(\frac{I^x}{I^{Ni}} \right)_{cal} = \frac{f_s^x \int_0^\infty (d\eta/dS)^x / N_0^x \exp(-S/\lambda_x) dS}{f_s^{Ni} \int_0^\infty (d\eta/dS)^{Ni} / N_0^{Ni} \exp(-S/\lambda_{Ni}) dS}$$

Comparison of IMFPs from EPES experiments at low energy region (under 200 eV)



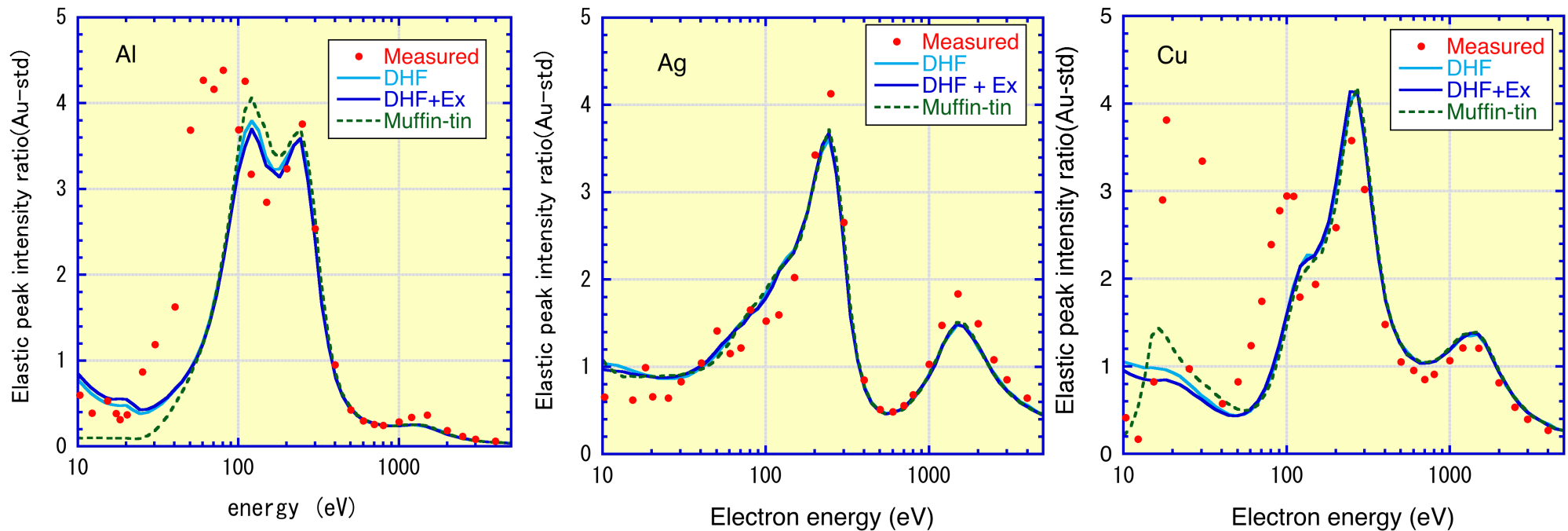
* surface excitation effect for EPES

* IMFP values of Ni STD at low energy

* electron exchange effect, correlation effect

EPI ratios of elemental solids (Au. Ref) vs. electron energy

SEE: $f = 1.0$ in the EPI calculations



>200 eV : differences of SEE among Al ,Ag, Cu and Au are small
-> similar energy dependence, small material dependence

< 100 eV : differences of measured and calculated EPIs are very large
-> SEE ? IMFP of ref. ? Exchange, correlation etc in IMFP calculation.

5. Summary

- We calculated IMFPs for 41 elemental solids and 30 compound semiconductors from experimental and calculated optical data for electron energies from 10 eV to 200 keV using relativistic FPA
- We obtained excellent ELF's from Wien2k and FEFF code for 30 compound semiconductors
- Relativistic Modified Bethe equation fits optical IMFPs well over 50 eV – 200 keV. Average RMS : 0.8% for elemental solids, 0.7% for semiconductors.
- Relativistic TPP-2M equation provides reasonable estimates of IMFPs over 50 eV – 200 keV. Average RMS : < 12% in both group.
: down to < 9% (except for graphite, diamond, Cs and BN)
- IMFPs from elastic-peak electron spectroscopy experiments generally agree well with optical IMFPs over 200 eV (up to 5keV)
- large deviation between calculated and measured EPI ratio (for Al/Au, Cu/Au)) under 100 eV
:SEE, electron exchange and correlation effect must be considered at low energy region.